Effects of prestress on a hyperelastic, anisotropic and compressible tube

Dr Edouard Diouf
Laboratoire Mathématiques et Applications
Université Assane Seck de Ziguinchor,
BP 523 Ziguinchor, Sénégal
ediouf@univ-zig.sn

Abstract: We consider a hyperelastic, compressible, prestress and circular tube subjected to finite torsion and axial stretch. The mechanical response of the material is describes by an Ogden strain energy function with unidirectional reinforcement. The nonlinear equations governing the boundary problem are solved numerically by using the Runge-Kutta method. The effects of the prestress on the stress distributions are presented and permit to study a prototype vascular prosthesis of small diameter.

Keys-words: hyperelastic, compressible, anisotropic, prestress, small diameter vascular prosthesis

———————————— ◆ ————————————

1. Introduction

The following article describes valuable techniques for fabricating devices deemed suitable for prosthetic applications in animals and humans. However, *in vivo* stability of the recommended constituent material is not completely demonstrated, and clinically important degenerative phenomena which may impact adversely on long-term safety are not addressed.
The design and fabrication of small diameter vascular prosthesis less than 6 mm which could assure a permanent functional service without the help of medicinal therapeutics, constitute a challenge subordinate to the necessity of well defining the fundamental characteristics of the ideal transplant [1].
The replacement of small-diameter blood vessels ($\leq$ 6mm) is a clinical situation Frequently encountered by vascular and cardiothoracic surgeons [2].
Thus, in most cases, the use of the autologous saphenous vein, which is considered
to be excellent autologous graft material in small diameter reconstructions [3], is the preferred solution. However, this vein is not available in one-third of patients, and the use of alternative prostheses becomes necessary. Artificial materials are then proposed and are currently represented by commercially available polyester prostheses.
Unfortunately, these biomaterials are not hemocompatible enough to allow a long-term
Patency rate (>5 years) and to be implanted without the administration of
An adequate anticoagulotherapy [3].
The mimic the arterial materials [4], the elastic properties of biomaterials have to be hyperelastic and anisotropic. Indeed, the mechanical properties of such biomaterials are extremely important when selecting a material for the fabrication of vascular prosthesis.
The reader could consult the works of How et al. [1] where the design requirement and the development of vascular grafts are investigated in details.
In this contribution, we propose a compressible hyperelastic model to simulate the mechanical behavior of a tubular structure. This is a prototype of a small-diameter vascular graft composed of a silicone matrix embedded by fibers.
Using experimental data [5], we show that the Ogden response can adequately represent the behavior of a silicone material. Furthermore, we show that such

a fiber-reinforced silicone material offers a high mechanical similarity to natural arterial material. In the theoretical approach, we investigate the Ogden response augmented with unidirectional reinforcing characterized by a single additional constitutive parameter for strength of reinforcement. Then, the mechanical behavior of a prestressed tube subjected to a combined torsion and axial stretch deformation is considered. The non-linear equations governing this problem are established by the Runge-Kutta method. The different deformations have been analyzed and are thought to result from certain local physiological conditions which should be supported by the stress distributions are then studied for different intensities of the prestress.

2. Method

2.1 Preliminaries

Consider a non-linearly elastic solid in its undeformed state. In a cartesian coordinate system, let $\mathbf{x} = (x_i)$ denote the coordinates of a particle in the undeformed state and $\mathbf{y} = (y_i)$ denote its coordinates in the deformed state. We will note the components of the deformation gradient $\mathbf{F}$, the left Cauchy-Green deformation tensor $\mathbf{B}$ and the right Cauchy-Green deformation tensor $\mathbf{C}$, by

$$\mathbf{F} = \frac{\partial y_i}{\partial x_j},\ \mathbf{B} = \mathbf{F}_{ik}\mathbf{F}_{jk},\ \mathbf{C} = \mathbf{F}_{ki}\mathbf{F}_{kj} \qquad (1)$$

Assuming that the material is transversely isotropic i.e. reinforced by fibers, the strain energy functional W will depend on four strain invariants as follows

$$I_1 = tr(\mathbf{B}),\ I_2 = tr(\mathbf{B}^*),\quad I_3 = J^2 = \det(\mathbf{B}), I_4 = \tau.\mathbf{C}.\tau \qquad (2)$$

where $\mathbf{B}^* = (\det(\mathbf{B}))\mathbf{B}^{-1}$ is the adjoint of $\mathbf{B}$, J is the local volume change and $\boldsymbol{\tau} = (\tau_i)$ is the preferential direction vector in the undeformed state to the transverse isotropic direction $\mathbf{t} = (t_i)$ in the deformed state by $\mathbf{t} = \mathbf{F}\boldsymbol{\tau}/\sqrt{I_4}$.

For transversely isotropic compressible materials and in the particular case of four strain invariants, the Cauchy stress tensor $\boldsymbol{\sigma}$ is given by

$$\sigma = \frac{2}{J}[(I_2W_2 + I_3W_3)\mathbf{I}_d + W_1\mathbf{B} - I_3W_2\mathbf{B}^{-1} + I_4W_4(\mathbf{t}\otimes\mathbf{t})], \qquad (3)$$

Where $\mathbf{I}_d$ denotes the identity tensor and $W_k = \partial W/\partial I_k, (k = 1,2,3,4)$.

Consider now an Ogden material reinforced in $\boldsymbol{\tau}$ direction [6, 7]

$$\sigma = \frac{2}{J}[(I_2W_2 + I_3W_3)\mathbf{I}_d + W_1\mathbf{B} - I_3W_2\mathbf{B}^{-1} + I_4W_4(\mathbf{t}\otimes\mathbf{t})], \qquad (4)$$

where the scalar μ_o is the usual constant shear modulus for infinitesimal deformations from the undeformed state. The constants (a_1, a_2, a_3) are dimensionless parameters and the constant a_4 and n represent respectively the density of reinforcement and the fiber stiffness. Also, from (3) and (4) yield the corresponding behavior law expressed as

$$\sigma = \frac{\mu_o}{J}[(a_1I_2 + a_2I_3 + \frac{a_3}{2})\mathbf{I}_d + \mathbf{B} - a_1I_3\mathbf{B}^{-1} + na_4I_4(I_4 - 1)^n(\mathbf{t}\otimes\mathbf{t})]. \qquad (5)$$

Let us examine a state of plane strain uniaxial stress parallel to the x_1-axis, $\sigma_{11} = F, \sigma_{22} = 0, \lambda_3 = 1$.

When the fibers are parallel to the de direction of loading $(\text{i.e.}\ \tau_1 = 1, \tau_2 = 0, \tau_3 = 0)$, it may readily be shown that the applied stress F and the transverse stretch λ_2 are related to the principal stretch $\lambda_1 = \Lambda$ as follows

$$\frac{F}{\mu_o} = (a_1+1)\frac{\Lambda}{\lambda_2} + (a_1+a_2)\Lambda\lambda_2 + \frac{a_3}{2}\frac{1}{\Lambda\lambda_2} + na_4\frac{\Lambda}{\lambda_2}(\Lambda^2-1)^{n-1}, \qquad (6)$$

with $\lambda_2 = \left[\frac{-a_3}{2((a_1+1)+(a_1+a_2)\Lambda^2}\right]^{1/2}$.

The engineering stress T is expressed as $T = F\lambda_2$.

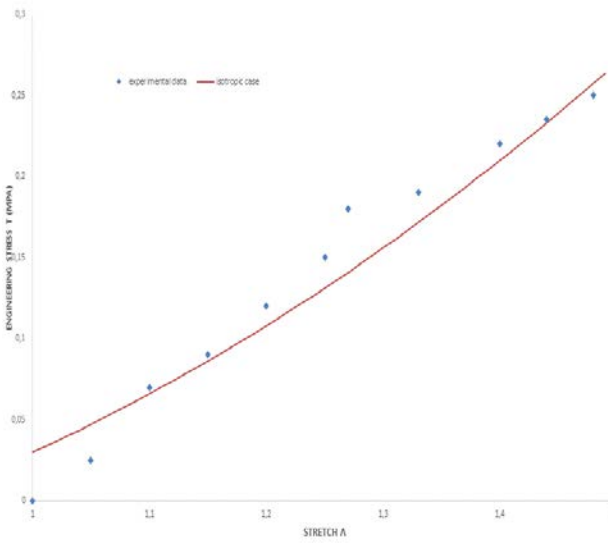

Fig.1 Mechanical response (stress vs stretch) of silicone material in plane uniaxial stress

Figure 1 shows the stress-stretch relation for the isotropic case and the comparison with the experimental results obtained on homogeneous silicone specimen.
The fit parameters that have been found $(a_1 = 0.25,\ a_2 = -0{,}02,\ a_3 = 3)$ and correspond to values which permit to approach measured data. We show clearly that, in tension, the isotropic model offers a close mechanical similarity to the silicone material.

2.2 Thick cylinder subjected to torsion and axial stretch

Consider a compressible and opened tube defined by the angle Θ_0 and made of a material des described by (4). Let us suppose that the tube undergoes two successive deformations. First including the closure and axial stretch of the tube which induce residual strains [8], and second including radial solicitations. The displacement is then prescribed by

$$r = r(R),\ \ \theta = \left(\frac{\pi}{\Theta_o}\right)\Theta + \Psi\Lambda Z,\ \ z = \lambda\Lambda Z, \tag{7}$$

where (R, Θ, Z) and (r, θ, z) are respectively the reference and the deformed coordinates of a material particle in a cylindrical system. Here Ψ is a twist angle per unloaded length, Λ and λ are axial stretch ratios (respectively, for the first and the second deformation). Let R_i and r_i denote respectively the inner surfaces of the cylinder in the reference state and in the deformed state (R_o and r_o are the outer surfaces).
A routine calculation gives the physical components of the $\mathbf{F}, \mathbf{B}$ and $\mathbf{C}$.

The four strain invariants I_1, I_2, I_3 and I_4 are given by

$$I_1 = \Lambda^2\lambda^2 + \Psi^2\Lambda^2 r(R)^2 + \left(\frac{\pi r(R)}{\Theta_0 R}\right)^2 + r'(R)^2,$$

$$I_2 = \Lambda^2\left(\lambda^2 + \Psi^2 r(R)^2\right)r'(R)^2 + \left(\lambda^2\Lambda^2 + r'(R)^2\right)\left(\frac{\pi r(R)}{\Theta_0 R}\right)^2,$$

$$I_3 = \left(\frac{\pi\lambda\Lambda r(R)}{\Theta_0 R}r'(R)\right)^2,$$

$$I_4 = \tau_R^2 r'(R)^2 + \tau_\Theta\left(\frac{\tau_\Theta \pi^2 r(R)^2}{\Theta_0^2 R^2} + \frac{\tau_Z \pi\Psi\Lambda r(R)^2}{\Theta_0 R}\right) + \tau_Z\left(\tau_Z\left(\Psi^2\Lambda^2 r(R)^2 + \Lambda^2\lambda^2\right) + \frac{\tau_\Theta \pi\Psi\Lambda r(R)^2}{\Theta_0 R}\right), \tag{9}$$

where $(\tau_R, \tau_\Theta, \tau_Z)$ are the components of the fibre direction in the undeformed configuration.
Using (5), it is easily follows that the stress components with respect to cylindrical coordinates are

$$\sigma_{rr}=\frac{\mu_0}{J}\left[\begin{array}{l}\frac{a_3}{2}+a_1I_2+a_2I_3+r'(R)^2\\ -\frac{a_1I_3}{r'(R)^2}+na_4\tau_R^2r'(R)^2(I_4-1)^{n-1}\end{array}\right],$$

$$\sigma_{r\theta}=\frac{\mu_0}{\Theta_0RJ}na_4\tau_Rr(R)r'(R)\left(\pi\tau_\Theta+\tau_Z\Psi\Lambda\Theta_0R\right)(I_4-1)^{n-1},$$

$$\sigma_{rZ}=\frac{\mu_0}{J}na_4\tau_R\tau_Z\lambda\Lambda r'(R)(I_4-1)^{n-1},$$

$$\sigma_{\theta\theta}=\frac{\mu_0}{J}\left[\begin{array}{l}\frac{a_3}{2}+a_1I_2+a_2I_3+\Psi^2\Lambda^2r'(R)^2+\left(\frac{\pi r(R)}{\Theta_0R}\right)^2\\ +n\,a_4(I_4-1)^{n-1}\left(\tau_Z\Psi\Lambda r(R)+\frac{\pi\tau_\Theta r(R)}{\Theta_0R}\right)^2-a_1I_3\left(\frac{\Theta_0R}{\pi r(R)}\right)^2\end{array}\right],$$

$$\sigma_{\theta z}=\frac{\mu_0}{J}\left[\begin{array}{l}\Psi\lambda\Lambda^2r(R)+na_4\tau_Z\lambda\Lambda(I_4-1)^{n-1}\left(\tau_Z\Psi\Lambda r(R)+\frac{\pi\tau_\Theta r(R)}{\Theta_0R}\right)+\\ a_1I_3\left(\frac{\Psi\Theta_0^2R^2}{\lambda\pi^2r(R)}\right)\end{array}\right],$$

$$\sigma_{zz}=\frac{\mu_0}{J}\left[\begin{array}{l}\frac{a_3}{2}+a_1I_2+a_2I_3+\lambda^2\Lambda^2+na_4\tau_Z^2\lambda^2\Lambda^2(I_4-1)^{n-1}\\ -a_1I_3\frac{\pi^2+\Psi^2\Lambda^2\Theta_0^2R^2}{\pi^2\Lambda^2\lambda^2}\end{array}\right]. \qquad (10)$$

From (5, 8) the equilibrium equations in the absence of body forces are reduced to

$$\frac{\mathrm{d}\sigma_{rr}}{\mathrm{d}r}+\frac{1}{r}(\sigma_{rr}-\sigma_{\theta\theta})=0,$$
$$\frac{\mathrm{d}\sigma_{r\theta}}{\mathrm{d}r}+\frac{2}{r}\sigma_{r\theta}=0$$
$$\frac{\mathrm{d}\sigma_{rz}}{\mathrm{d}r}+\frac{\sigma_{rz}}{r}=0.$$

Substituting (10) into (11.a), we obtain the nonlinear differential equation

$$f_1(R,r,r')r''(R)+f_2(R,r,r')r'(R)^3+$$
$$f_3(R,r,r')r'(R)^2+f_4(R,r,r')=0,$$

where f_i, $i=1,2,3,4$ are continuous for $R\in[R_i,R_o]$.

Finally to determine $r(R)$, we impose the boundary conditions such as $r(R_i)=R_i$ and $r(R_o)=R_o$.

Thus, the boundary-value problem consist of equations (11) with the boundary conditions, where the torsion angle Ψ and axial stretch Λ are given.

3. Results and discussion

The boundary value problem is numerically solved by using the Runge-Kutta method of 4th order and a complementary iterative procedure, where we take 100 points on the radial coordinate and check the circumferential stretch ration against the boundary condition until it is satisfied. Therefore, we consider the case where a tube made of silicone material is reinforced with axial fibers. The tube represents a prototype of small diameter vascular prosthesis [5] and is subjected to fixed twisting angle $\Psi=30°$, axial stretch $\Lambda=1{,}3$, the density of reinforcement $a_4=0{,}75$ and different intensities of the prestress defined by the values of the parameter $\Theta_0=\{45°,60°,90°,120°\}$.

We note two step in Figure 2. First the circumferential stress decreases as $R\in\left[R_i,\frac{R_o-R_i}{2}\right]$, then it grows rapidly $R\in\left[\frac{R_o-R_i}{2},R_o\right]$ as for $\Theta_o=45°$.

Note also that $\sigma_{\theta\theta}$ is very large when R approaches R_o. (11)

This could be explained by the fact, the residual stresses are much higher on the outer surface of the tube because of the opening angle.

In Figure 3, we note that the circumferential stress increases with Θ_o but all these circumferential stress are decreasing.

It should be noted the very large gap between Figure 2 and Figure 3.

For an angle opening $\Theta_o=45°$, $\sigma_{\theta\theta}$ is around 100 MPa while it is in the order of 2 MPa for $\Theta_o=60°,90°,120°$.

When R approach of R_o for an angle $\Theta_o=45°$, the circumferential stress grows

very rapidly, while it decreases for angles $\Theta_o = 60°, 90°, 120°$.

We can conclude in these cases, unless the opening angle is, the more $\sigma_{\theta\theta}$ is great. There is more stress concentration for small angles than for high angles.

In Figure 4, we seek to establish the influence of the parameter n, the fiber stiffness, in the circumferential stress distributions.

It appears that, for $n = 2$ or $n = 3$, and $\Theta_o = 45°$, the circumferential stress decreases. Its maximum value is in the order of 1,8 MPa.

We note that for $n = 4$ in Figure 2, the stress $\sigma_{\theta\theta}$ is very large so that it is slow for for $n = 2$ or $n = 3$. By comparing figures 2 and 4, we note that the fiber stiffness has a great influence in the circumferential stress distributions. In terms of maximum value, the function $\sigma_{\theta\theta}$ is much larger than the fiber stiffness is high.

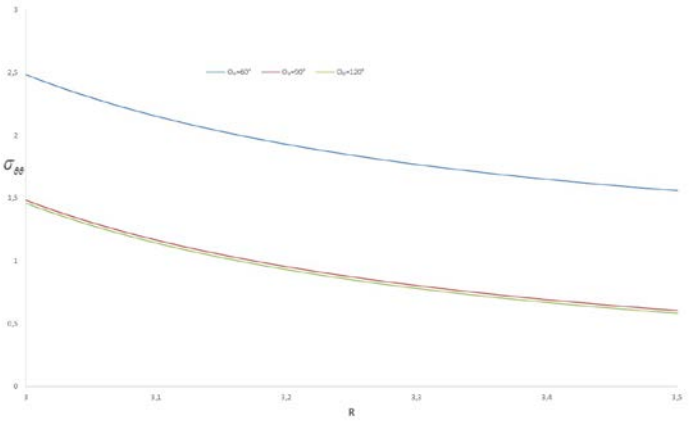

Fig.3 Circumferential stress distributions vs radius for different angles $\Theta_0, n = 4$

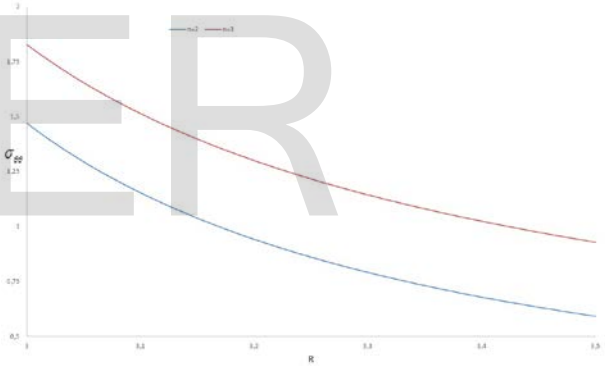

Fig.4 Circumferential stress distributions vs radius for $\Theta_0 = 45°, n = 2$ and $n = 3$.

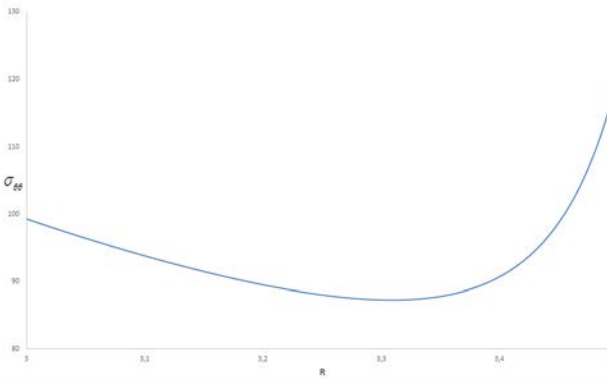

Fig.2 Circumferential stress distributions vs radius for $\Theta_0 = 45°, n = 4$

References

[1] How T.V,Guidoin R., young S.K.: Engineering design of vascular prostheses. J.Eng.Med., Part H., p.61-71, (1992).

[2] Abbott, W.M.,Vignati,J.J.: Prosthetic graft when are reasonable alternative?
Semin. Vasc.Surg.8, 235-245 (1995).

[3] Greenwald S.E., Berry C.L.: Improving vascular grafts: the important of the mechanical and

haemodynamic properties. J. Pathol. 190,292-299, (2000).

[4] Fung Y.C.:Biomechanics, Mechanical properties of living tissues, 2nd edition, Springer-Verlag.New-York, (1993).

[5] Cheref M.: Approche mécanique à la conception d'une prothèse vasculaire de petit diameter, PHD Thesis, université Paris 12 Val de Marne (1998).

[6] Diouf E., Exact solution of a problem of dynamic deformation and nonlinear stability of a problem with a Blatz-Ko mateial, IJSER. Vol.3, Isuue 2, (2012).

[7] Spencer AJ.M.: Continuum theory of the mechanics of fibre-reinforced composites, Springer, New-York, (1984).

[8] Diouf E., Modélisation hyperélastique, anisotrope, compressible et dynamique d'une structure tubulaire épaisse,PHD Thesis, université Paris 12 Val de Marne (2005).